

Turnover of branched actin filament networks by stochastic fragmentation with ADF/cofilin

Anne-Cécile Reymann^{a,*}, Cristian Suarez^{a,*}, Christophe Guérin^a, Jean-Louis Martiel^a, Christopher J. Staiger^{b,c}, Laurent Blanchoin^a, and Rajaa Boujemaa-Paterski^a

^aLaboratoire de Physiologie Cellulaire & Végétale, Institut de Recherches en Technologies et Sciences pour le Vivant (iRTSV), Centre National de la Recherche Scientifique/Commissariat à l'énergie atomique et aux énergies alternatives/Institut National de la Recherche Agronomique/Université Joseph Fourier (CNRS/CEA/INRA/UJF), Grenoble 38054, France; ^bDepartment of Biological Sciences and ^cThe Bindley Bioscience Center, Purdue University, West Lafayette, IN 47907-2064

ABSTRACT Cell motility depends on the rapid assembly, aging, severing, and disassembly of actin filaments in spatially distinct zones. How a set of actin regulatory proteins that sustains actin-based force generation during motility work together in space and time remains poorly understood. We present our study of the distribution and dynamics of Arp2/3 complex, capping protein (CP), and actin-depolymerizing factor (ADF)/cofilin in actin "comet tails," using a minimal reconstituted system with nucleation-promoting factor (NPF)-coated beads. The Arp2/3 complex concentrates at nucleation sites near the beads as well as in the first actin shell. CP colocalizes with actin and is homogeneously distributed throughout the comet tail; it serves to constrain the spatial distribution of ATP/ADP-P_i filament zones to areas near the bead. The association of ADF/cofilin with the actin network is therefore governed by kinetics of actin assembly, actin nucleotide state, and CP binding. A kinetic simulation accurately validates these observations. Following its binding to the actin networks, ADF/cofilin is able to break up the dense actin filament array of a comet tail. Stochastic severing by ADF/cofilin loosens the tight entanglement of actin filaments inside the comet tail and facilitates turnover through the macroscopic release of large portions of the aged actin network.

Monitoring Editor
Fred Chang
Columbia University

Received: Jan 20, 2011
Revised: May 12, 2011
Accepted: May 17, 2011

INTRODUCTION

Cellular motility is a fundamental process essential for embryonic development, immune responses, wound healing, and neuronal growth cone migration (Pollard *et al.*, 2000). During motility, the rapid assembly and disassembly of actin networks provide the driving

This article was published online ahead of print in MBoc in Press (<http://www.molbiolcell.org/cgi/doi/10.1091/mbc.E11-01-0052>) on May 25, 2011.

*These authors contributed equally to this work.

Address correspondence to: Laurent Blanchoin (laurent.blanchoin@cea.fr) or Rajaa Boujemaa-Paterski (rajaa.paterski@cea.fr).

Abbreviations used: ABP, actin-binding protein; ADF, actin-depolymerizing factor; BSA, bovine serum albumin; CP, capping protein; DTT, dithiothreitol; Ena/VASP, Enabled/vasodilator-stimulated phosphoprotein; FRAP, fluorescence recovery after photobleaching; GST-pWA, glutathione-S-transferase-polyproline verproline homology acidic C-terminus regions of human Wiskott-Aldrich syndrome protein (WASp); NPF, nucleation-promoting factor; TCEP, Tris(2-carboxyethyl)phosphine.

© 2011 Reymann *et al.* This article is distributed by The American Society for Cell Biology under license from the author(s). Two months after publication it is available to the public under an Attribution-Noncommercial-Share Alike 3.0 Unported Creative Commons License (<http://creativecommons.org/licenses/by-nc-sa/3.0>). "ASCB®," "The American Society for Cell Biology®," and "Molecular Biology of the Cell®" are registered trademarks of The American Society of Cell Biology.

force that deforms the plasma membrane (Pollard and Cooper, 2009). Upon signaling, site-directed actin assembly at the leading edge of migrating cells depends primarily on the activation of the Arp2/3 complex, one of the three known actin nucleators in eukaryotes (Welch *et al.*, 1998; Machesky *et al.*, 1999; Rohatgi *et al.*, 1999; Svitkina and Borisy, 1999; Pollard and Borisy, 2003; Goley and Welch, 2006; Rouiller *et al.*, 2008). The activated complex triggers the rapid de novo assembly of a rigid and highly cross-linked actin filament array called the "dendritic network" (Mullins *et al.*, 1998; Machesky *et al.*, 1999; Blanchoin *et al.*, 2000a; Achard *et al.*, 2010). To efficiently convert the chemical energy provided by ATP hydrolysis within an actin filament into mechanical forces, rapid assembly of the actin network must be 1) localized underneath the plasma membrane (Rohatgi *et al.*, 1999) and 2) supplied with a large reservoir of actin monomers (Pantaloni *et al.*, 2000; Pollard *et al.*, 2000). Selective recruitment of nucleation-promoting factors (NPFs) to the sites of signaling (Chhabra and Higgs, 2007; Pollard and Cooper, 2009), followed by the rapid arrest of fast-growing barbed ends of actin filaments by capping protein (CP; Schafer *et al.*, 1996; Yamashita *et al.*, 2003; Kim *et al.*, 2004), prevents the expansion of Arp2/3-branched

actin meshwork away from the load (membrane). This ensures the formation of a sufficiently rigid and branched meshwork that pushes the plasma membrane forward (Iwasa and Mullins, 2007; Achard et al., 2010). Disassembly of the aged actin network is then required to maintain the large cellular reservoir of polymerizable actin monomers, and is achieved through fragmentation by actin-binding proteins (ABPs), the most important of which is actin-depolymerizing factor (ADF)/cofilin (Pollard et al., 2000; Chan et al., 2009; Bernstein and Bamberg, 2010). ADF/cofilin is known to bind preferentially to the aged, thus ADP-loaded, part of the actin filament (Blanchoin and Pollard, 1999). This changes the structure and mechanical properties of ADP-loaded actin filaments (McGough et al., 1997; McCullough et al., 2008) and promotes fragmentation (Maciver et al., 1991; Blanchoin and Pollard, 1999; Michelot et al., 2007; De La Cruz, 2009) into small and depolymerizing pieces by a mechanism called “stochastic dynamics” (Michelot et al., 2007; Chan et al., 2009). The general features of this process were recently observed in vivo (Staiger et al., 2009). Alternatively, rather than depolymerizing, short cofilin-generated fragments or oligomers can contribute to actin filament elongation in vivo (Okreglak and Drubin, 2010). Finally, ADF/cofilin binding and severing activities are regulated by molecular partners, including Aip1 and/or coronin that promote efficient actin monomer recycling (Okada et al., 2006; Kueh et al., 2008; Gandhi et al., 2009; Bernstein and Bamberg, 2010). The biochemical properties of most ABPs are individually well characterized in bulk solution or in reconstituted minimal systems (Loisel et al., 1999; Pollard and Borisy, 2003). However, the coordination of their actions in space and time, necessary to precisely choreograph actin turnover and organization and to generate proper network dynamics and mechanics, remains poorly documented (Brieher et al., 2006; Reymann et al., 2010).

To answer the question of how a minimal set of purified ABPs coordinate their functions to promote force production and actin-based motility, we examined the spatiotemporal distribution of the Arp2/3 complex, CP, and ADF/cofilin along the actin “comet tail” of motile particles in vitro. We found that the Arp2/3 complex is concentrated near the nucleation sites to initiate branched actin networks, and remains attached to the actin tail after it detaches from the nucleation sites. CP distributes homogeneously throughout the actin network of the comet tail. Conversely, ADF/cofilin binds preferentially at the rear of the comet tail, with a spatial distribution consistent with the state of the nucleotide in these aged parts of the actin tail, and induces massive breakage of the network into small and drifting pieces. Thus the macroscopic stochastic dynamics modulated by ADF/cofilin fragmentation of the aged part of the actin filament network arises as a major event during the fast actin disassembly necessary to maintain a steady dynamical regime during force production.

RESULTS

Arp2/3 complex and CP are continuously incorporated in elongating actin filament networks during actin-based motility

To image the spatiotemporal distribution of the Arp2/3 complex and CP within propulsive actin networks, we reconstituted motility of functionalized polystyrene beads in a physiologically relevant system prepared from profilin–G-actin-buffered medium containing the Arp2/3 complex and CP, in the absence of ADF/cofilin. Alternatively, we used a fluorescently labeled version of these proteins without detecting any changes in the rate of bead motility, indicating that the fluorescent proteins behave similarly to the unlabeled proteins (Figures 1 and 2). The velocity of bead propulsion recorded was -0.4 – 0.6 $\mu\text{m}/\text{min}$. After 4–5 min of polymerization, an actin gel nucleated on the surface of beads coated with GST-pWA, which is a

nucleation-promoting factor, broke symmetry, propelled the bead forward, and initiated a propulsive actin comet tail (van der Gucht et al., 2005). As a first step, we followed the real-time incorporation of fluorescently labeled Arp2/3 complex into these actin networks (Figure 1A). A line scan of fluorescence intensity along the diameter of the beads toward the center of the comet tail (Figure 1A, dashed line) allowed us to visualize the relative amounts of Arp2/3 complex incorporated over time during the establishment of the motility (Figure 1A). We found that the Arp2/3 complex was concentrated at the surface of beads, where it is recruited by GST-pWA and activated to initiate new-branched actin filaments before being released (Figure 1A). This is consistent with its transient activation through the formation of a ternary complex, NPF–Arp2/3 complex–actin filament (Martin et al., 2006; Achard et al., 2010). After release, the Arp2/3 complex was sparsely present throughout the whole actin array, but was markedly more abundant in the first actin shell (Figure 1A, middle). This is in agreement with our recent findings on the assembly of a dense actin shell prior to symmetry breaking and motility (Achard et al., 2010).

We investigated next, the spatiotemporal incorporation of actin and CP within the actin-branched network by following simultaneously their localization with Alexa Fluor 488-CP and Alexa Fluor 568-actin (Figure 1B and Movie S1). We found that CP was homogeneously distributed along the comet tail and colocalizes with actin (Figure 1B), and is in agreement with previous reports of its biochemical properties and its association with elongating branched filaments in vitro (Achard et al., 2010). Biochemical characterization in vitro has established that CP binds the fast-growing barbed-end of actin filaments with high-affinity (Schafer et al., 1996; Yamashita et al., 2003; Kim et al., 2004) and blocks dynamics (Cooper and Schafer, 2000). This distribution of CP is also consistent with the autocatalytic nucleation process of actin networks mediated by the Arp2/3 complex. Continuous generation of free barbed ends and their rapid capping by CP leads to the formation of a rigid and highly cross-linked actin filament array responsible for production of propulsive forces. Concomitant with the dense localization of Arp2/3 complex in the actin shell formed prior to symmetry breaking, we also found a higher fluorescence of CP and actin in this region (Figure 1B). This demonstrates that the formation of the first actin shell requires a highly dense network of actin, Arp2/3 complex and CP (van der Gucht et al., 2005). During the ensuing actin-based motility, the network was not as dense and these three proteins were less abundant (Figure 1). Following this initial investigation on the localization of proteins involved in building the protrusive actin network, we focused our attention on the spatiotemporal localization of ADF/cofilin, a protein necessary for network disassembly.

ADF/cofilin associates preferentially with the aged part of the comet tail and accumulates over time

ADF/cofilin is a key factor involved in the recycling of actin monomers from polymerized networks and therefore renders them available for actin assembly and force production (Pollard et al., 2000). To characterize the macroscopic distribution of ADF/cofilin within the dynamic branched actin network, we followed the spatial and temporal distribution of ADF/cofilin in the actin comet tail by simultaneously tracking the fluorescence associated with Alexa Fluor 488-ADF/cofilin and Alexa Fluor 568-monomeric actin. We found that the recruitment of ADF/cofilin was delayed compared with the polymerization of actin networks around motile beads (Figure 2, A and D, and Supplemental Movie S2). Importantly, we showed that ADF/cofilin was excluded from the actin network during the early stage of actin assembly following symmetry-breaking

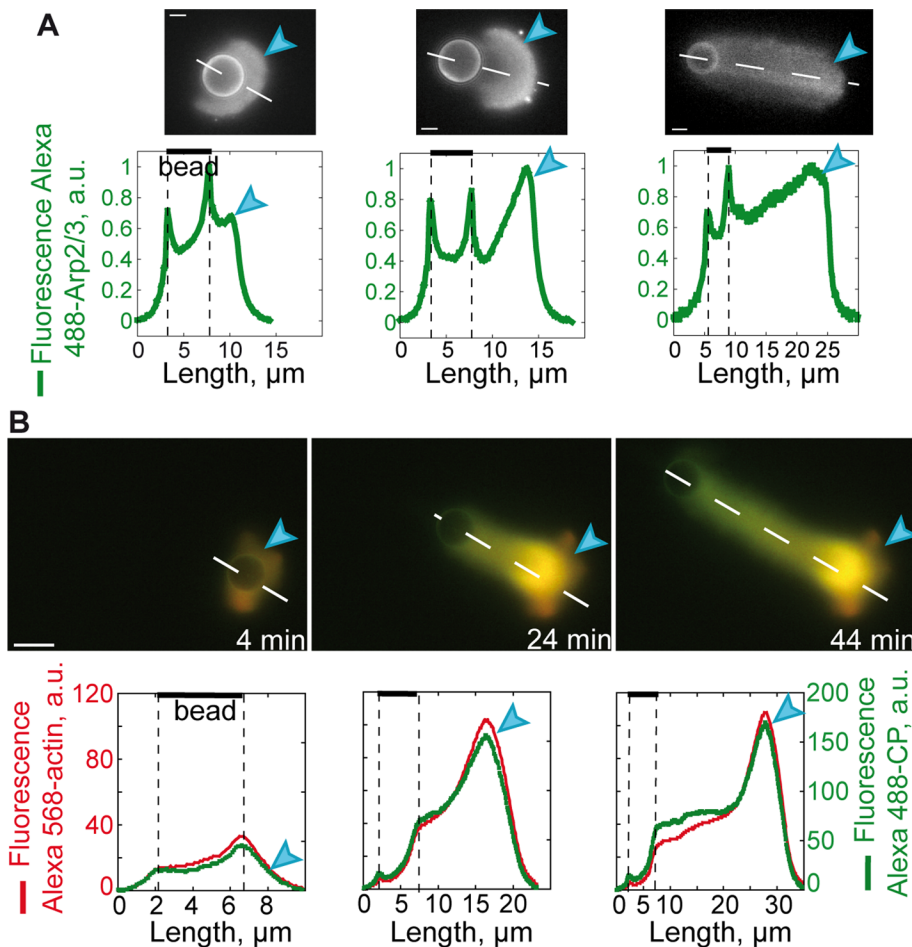


FIGURE 1: Arp2/3 complex and CP distribute homogeneously within the actin network during actin assembly. GST-pWA-coated beads were added to a motility medium containing 4 μM Alexa Fluor 568-actin monomers, 12 μM profilin, and (A) 210 nM Alexa Fluor 488-Arp2/3 complex, 25 nM CP, or (B) 150 nM Arp2/3 complex, 45 nM Alexa Fluor 488-CP. Images were taken at the indicated times during polymerization. Alexa Fluor 488 is colored in green and Alexa Fluor 568 in red. In (A) different motile beads were imaged after 30 min of actin assembly, and in (B) a montage of time-lapse images of a motile bead taken at 20-min intervals shows the comet tail formation. Line scans of the fluorescence intensities taken along the actin gel, as indicated by the dashed curves, are displayed under each corresponding image. For easier comparison in (A), we normalized the fluorescence by the integrated fluorescence of each image. Scale bar: 5 μm . (See also Movie S1.)

events (for at least 4 min; Figure 2, A and D). After 26 min of actin polymerization, ADF/cofilin was incorporated at the distal or aged part of the comet tail but remained excluded from the proximal or young part (Figure 2A). Quantification of the fluorescence ratio of ADF/cofilin to actin filaments in the comet tail demonstrates a dual process for ADF/cofilin incorporation within the actin network (Figure 2C). First, at a given time the concentration of ADF/cofilin increased gradually in space, from the proximal or young to the rear or aged part of the tail. Second, the concentration of ADF/cofilin increased gradually over time along the comet tail by enhancing the gradient already established along the actin network (Figure 2C). Because we confined the activation of Arp2/3 complex to the surface of NPF-coated beads, the newly polymerized zone is located near the bead. We propose that the spatiotemporal distribution of ADF/cofilin in the comet tail is modulated by the nucleotide state of the actin networks. Moreover, we followed the spatiotemporal incorporation of ADF/cofilin throughout dynamic actin networks in the absence of CP, and found that ADF/cofilin binding is

similarly governed by the biochemical state of actin-bound nucleotides of reconstituted parallel networks (Supplemental Figure S1 and Movie S3).

Biochemical studies have previously reported that kinetics of ATP hydrolysis along an actin filament occurs on a timescale of seconds, whereas that of the phosphate release happens on a timescale of minutes (Pollard *et al.*, 2000). Moreover, ADF/cofilin exhibits differential binding along the actin filament, with strong binding to ADP-loaded zones (K_d of 0.3 μM) and weak binding to ATP- or ADP- P_i -loaded zones ($K_d \approx 20 \mu\text{M}$; Carlier *et al.*, 1997; Blanchoin and Pollard, 1999).

We therefore measured the evolution over time of the ADF/cofilin exclusion zone in our system. We defined the exclusion zone as the area where ADF/cofilin is excluded from the actin tail, which is the region enriched in ATP- or ADP- P_i -loaded actin subunits. Remarkably, we found that ADF/cofilin exclusion zone length is nearly constant during propulsion. The length of the ADF/cofilin-free portion was $3.8 \pm 0.7 \mu\text{m}$ during 50 min (Figures 2A and 3C). Moreover, the exclusion zone length dropped rapidly and was abolished as soon as bead motility ceased (Figures 2B and 3C). Furthermore, exclusion zone length was sensitive to ADF/cofilin concentration (Figures 2, D and E, and 3D). Indeed, increasing the concentration of ADF/cofilin twofold resulted in an increase of the ratio of ADF/cofilin to actin along the comet tail over time (Figure 2, D and F). Consequently, the length of the exclusion zone of ADF/cofilin decreased by a factor of two, and was $2.2 \pm 0.6 \mu\text{m}$ during 30 min (Figures 2D and 3D). Interestingly, we noted that increasing the ADF/cofilin concentration enhanced bead motility; we recorded mean velocities of 0.3 or

0.5 $\mu\text{m}/\text{min}$ for ADF/cofilin concentrations of 0.3 and 0.6 μM , respectively (Figure 2, B and E).

Kinetic modeling accounts for the spatiotemporal incorporation of ADF/cofilin throughout expanding branched networks

The above results supported ADF/cofilin binding either to branched or to parallel actin networks concomitant with the chemical state of actin-bound nucleotide. Therefore, to understand mechanistically the distribution of ADF/cofilin along the growing actin comet tails, we developed a mathematical model that includes all the chemical reactions controlling the interaction of ADF/cofilin with actin filaments (Figure 3 and Supplemental Data). This model is based on the kinetics of actin assembly in the presence of profilin, the kinetics of ATP hydrolysis and phosphate release from actin filaments, and the kinetics of CP incorporation controlling actin filament length within branched actin networks. Moreover, we took into account the kinetics of interaction of ADF/cofilin with actin filaments, as well

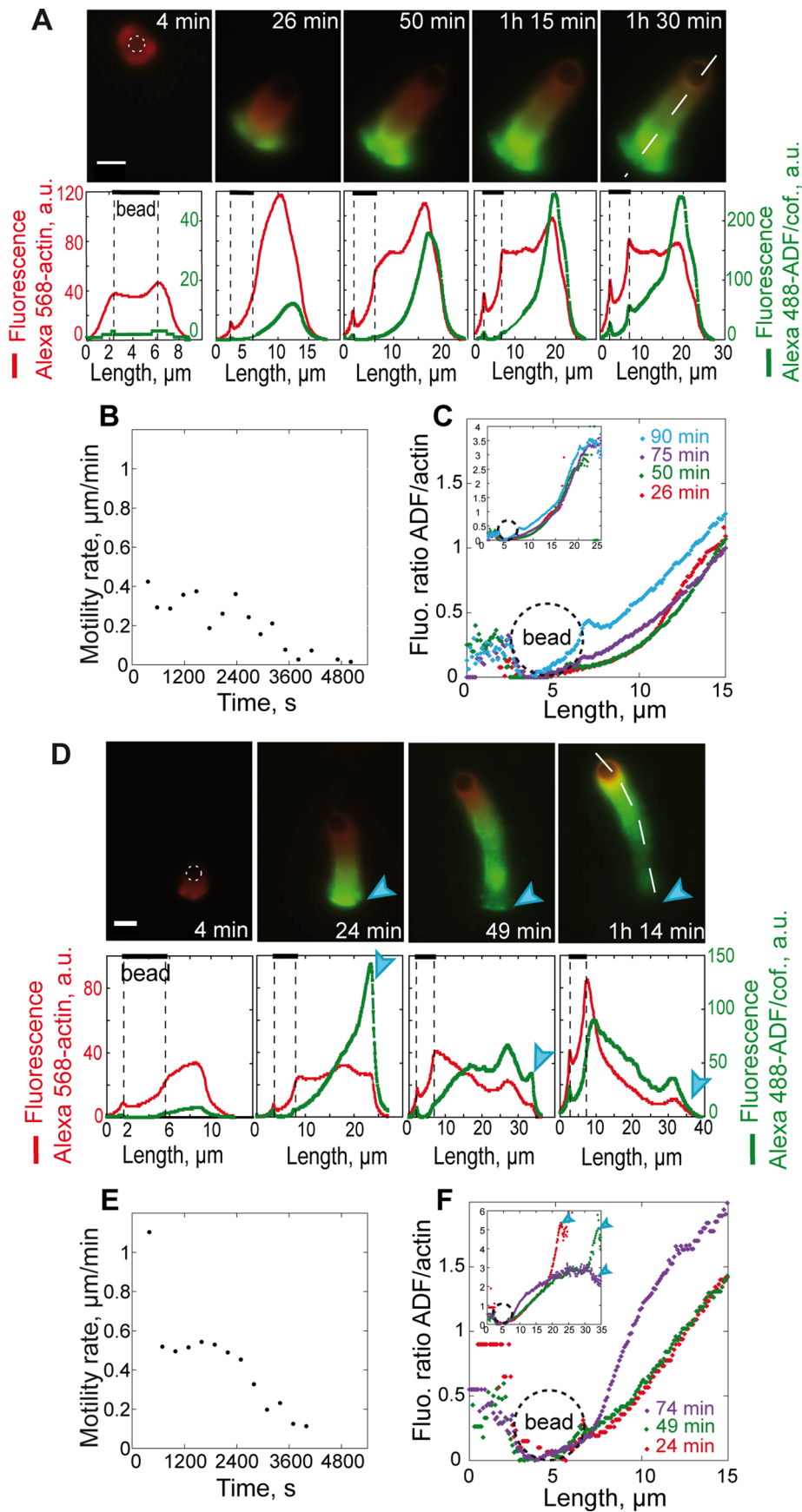


FIGURE 2: ADF/cofilin is progressively recruited to the actin comet tail during reconstituted bead motility. GST-pWA-coated beads were added to a motility medium containing 12 μM profilin, 4 μM Alexa Fluor 568-actin monomers, 150 nM Arp2/3 complex, 25 nM CP, and

as the subsequent acceleration (19-fold greater) of the phosphate release from neighboring subunits induced after ADF/cofilin binding (Figure 3 and Supplemental text; Blanchoin and Pollard, 1999).

In agreement with the experimental results, the kinetic reactions incorporated into the mathematical model could account for the aging of the actin network assembled in the absence or presence of ADF/cofilin (Figure 3 and Movie S4). In the absence of ADF/cofilin, and in the presence of actin and CP, the elongation zone of actin filaments was restricted to the bead vicinity. Additionally, the actin network underwent aging and the ADP-loaded region spread along the assembled network (Figure 3A). When ADF/cofilin was introduced, the kinetic model demonstrated that ADF/cofilin is gradually incorporated and enriched in the aged part of the actin tail, where it is presumed to induce severing of actin filament networks (Figure 3B; Blanchoin and Pollard, 1999). Remarkably, the simulated and experimental ADF/cofilin exclusion zone evolved similarly throughout actin network polymerization and bead motility (Figure 3, C and D). These results demonstrated that in our reconstituted system the spatiotemporal incorporation of ADF/cofilin within a polymerizing actin network is governed by kinetics.

ADF/cofilin fragments short actin filaments in the Arp2/3-mediated networks of propulsive comet tails

ADF/cofilin induces structural remodeling of branched networks in vitro by reducing the affinity of actin filaments for Arp2/3 complex and by destabilizing branches (Blanchoin

(A) 0.3 μM Alexa Fluor 488-ADF/cofilin or (D) 0.6 μM Alexa Fluor 568-ADF/cofilin. Images were taken at the indicated times during polymerization and analyzed as in Figure 1. Blue arrowheads indicate the site of abundant binding of ADF/cofilin and its abrupt dissociation due to the subsequent actin network fragmentation. Scale bar: 5 μm . (B and E) A time course of motility rates during actin comet tail formation was measured. (C and F) Line scans of the fluorescence intensities taken along the actin network, as indicated by the dashed lines in D, were analyzed for the different times of acquisition (as in Figure 1). Graphs represent the ratio of the fluorescence intensity for ADF/cofilin to that of actin at different times. A zoom of the vicinity around the bead is presented, whereas the inset shows the entire ratio of the full actin network. (See also Movies S2 and S3.)

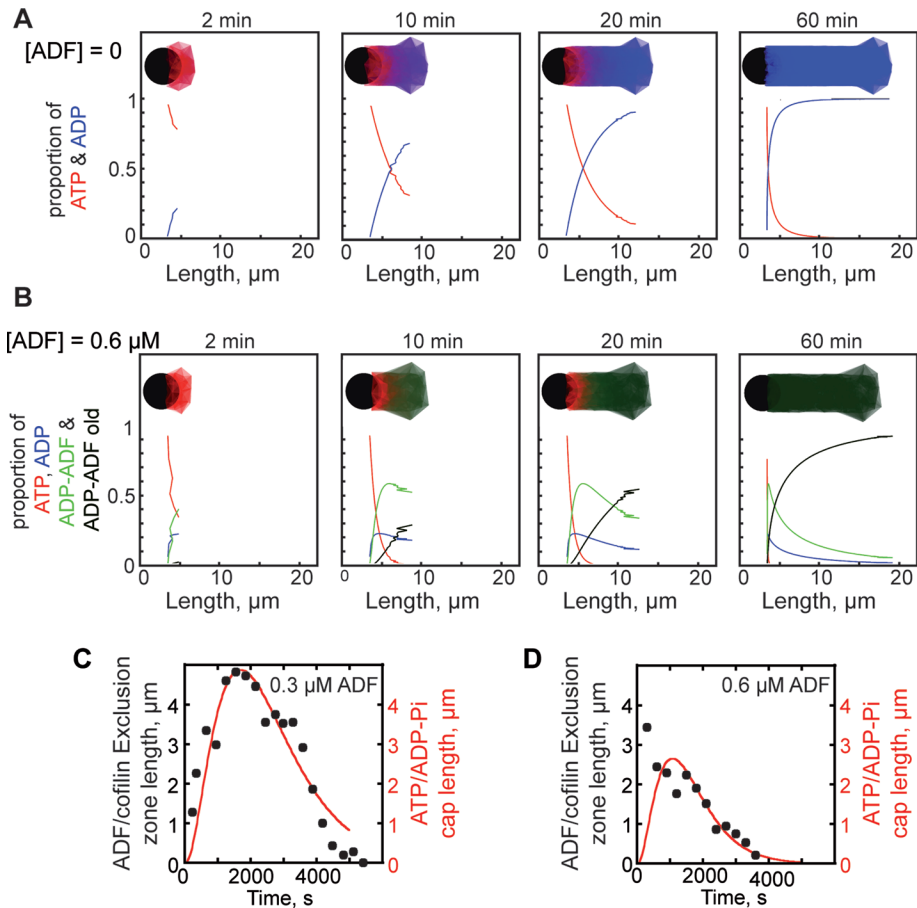


FIGURE 3: Kinetic modeling of ADF/cofilin recruitment within the comet tail. *In silico* reconstitution of the elongation of the Arp2/3-mediated actin branched network according to the kinetic model (Supplemental Data). (A and B) The graphs represent a montage of the evolution over time of the ratio of ATP- and ADP-loaded actin subunits within the simulated network assembled in the presence of $4 \mu\text{M}$ of profilin-actin complex, 25 nM CP, and ADF/cofilin as indicated. The ATP and ADP-P_i states of the nucleotide were incorporated into one, and named ATP. Simulations of the elongating comet tail were drawn and positioned with the front bead edge aligned with the origin of x-axis and the rear one with the interface bead/actin network. The color-coding of the comet tail corresponds to that of the curves. (B) Given the acceleration of P_i release on actin subunits by ADF/cofilin and the higher affinity for ADP-loaded subunits, the proportion of the ADP-loaded subunits diminished in favor of both ADP-ADF-loaded subunits and old ADP-ADF-loaded ones. The latter population accounted for severing by ADF/cofilin. (C) Superimposition of predicted ATP/ADP-P_i cap lengths (line) and experimental ADF/cofilin exclusion zones measured in Figure 2, A and D, respectively (dots); experimentally, the cap length, i.e., the zone of exclusion of ADF/cofilin, was represented by the red zone in the comet tail (Figure 2, A and D). (See also Movie S4.)

et al., 2000a; Chan *et al.*, 2009). At a low occupancy of filaments, it severs actin polymers, presumably because of torsion stress that accumulates at the interface between bare and ADF/cofilin-decorated regions of short actin filaments (De La Cruz, 2005; Andrianantoandro and Pollard, 2006; Suarez *et al.*, 2011). We therefore asked whether ADF/cofilin severing activity still occurs within actin networks rendered rigid and highly branched by the presence of CP, which significantly shortens the length of filament branches and increases the branch density (Blanchain *et al.*, 2000a; Achard *et al.*, 2010).

Line scans of fluorescence intensity for both labeled actin (red) and ADF/cofilin (green) taken along the comet tail at different times of actin polymerization revealed a shoulder in the actin curves (Figure 2, A and D). This heterogeneity in the actin concentration along the comet tail is consistent with the initial construction of a dense actin shell prior to symmetry breaking (Achard *et al.*, 2010). This

shoulder was observable during the early time course of bead motion (before 50 min) in the presence of a low concentration of ADF/cofilin but became progressively reduced thereafter, and disappeared after 1 h 30 min (Figure 2A), in agreement with the CP mean fluorescence along the tail (Figure S2). In the presence of a twofold increase in the concentration of ADF/cofilin, the amount of actin filaments was drastically reduced within the last 10 μm of the comet tail (Figure 2D, red curve: decreased regime) concurrent with the drop of ADF/cofilin amount in the same region of the comet (Figure 2D, green curve: decreased regime). One explanation for this reduction is that actin filaments in the comet tail are being disassembled due to the fragmentation activity of ADF/cofilin, similar to that observed *in vitro* for single growing actin filaments (Michelot *et al.*, 2007) or for branched actin networks (Blanchain *et al.*, 2000a; Chan *et al.*, 2009).

To address this question, we quantified the ADF/cofilin-mediated severing of actin filament branched arrays during motility. Based on the high affinity of CP for free barbed ends of actin filaments (K_d of 0.1 nM ; Schafer *et al.*, 1996), and assuming that CP binds to ADF/cofilin-severed ends with the same affinity, we used CP as a marker to estimate the amount of barbed ends present within an actin network. Thus, by comparing the amount of CP in propulsive comet tails, in the presence and absence of ADF/cofilin, we could estimate the extent of filament fragmentation in the dense networks. We used fluorescence recovery after photobleaching (FRAP) experiments on Alexa Fluor 488-CP incorporated in the comet tail during bead motility, with or without ADF/cofilin, to quantify the dynamics of CP within the propulsive actin network. A well-defined zone of the actin comet tail away from the bead center was bleached using a local intense laser illumination (Figure 4, B and C, and Movie S5).

Taking into account the photodamage due to the laser illumination (Figures 4A and S3 and Supplemental Data), we quantified the severing activity of ADF/cofilin in branched actin networks responsible for bead propulsion. During experiments conducted in the absence of ADF/cofilin, we determined the rate constant for slow fluorescence recovery corresponding to the dissociation rate constant of CP from the barbed ends of actin filaments to be $0.0015 \pm 0.0002 \text{ s}^{-1}$. This value is comparable to published values for CP k_{off} determined by other methods (Schafer *et al.*, 1996; Kuhn and Pollard, 2007). Interestingly, the presence of ADF/cofilin induced an increase in the amplitude of the rapid fluorescence recovery after photobleaching (Figure 4D). This demonstrated that ADF/cofilin fragments the actin networks, leading to the creation of free barbed ends that are rapidly capped by free CP present in the medium. Using the association rate constant reported previously

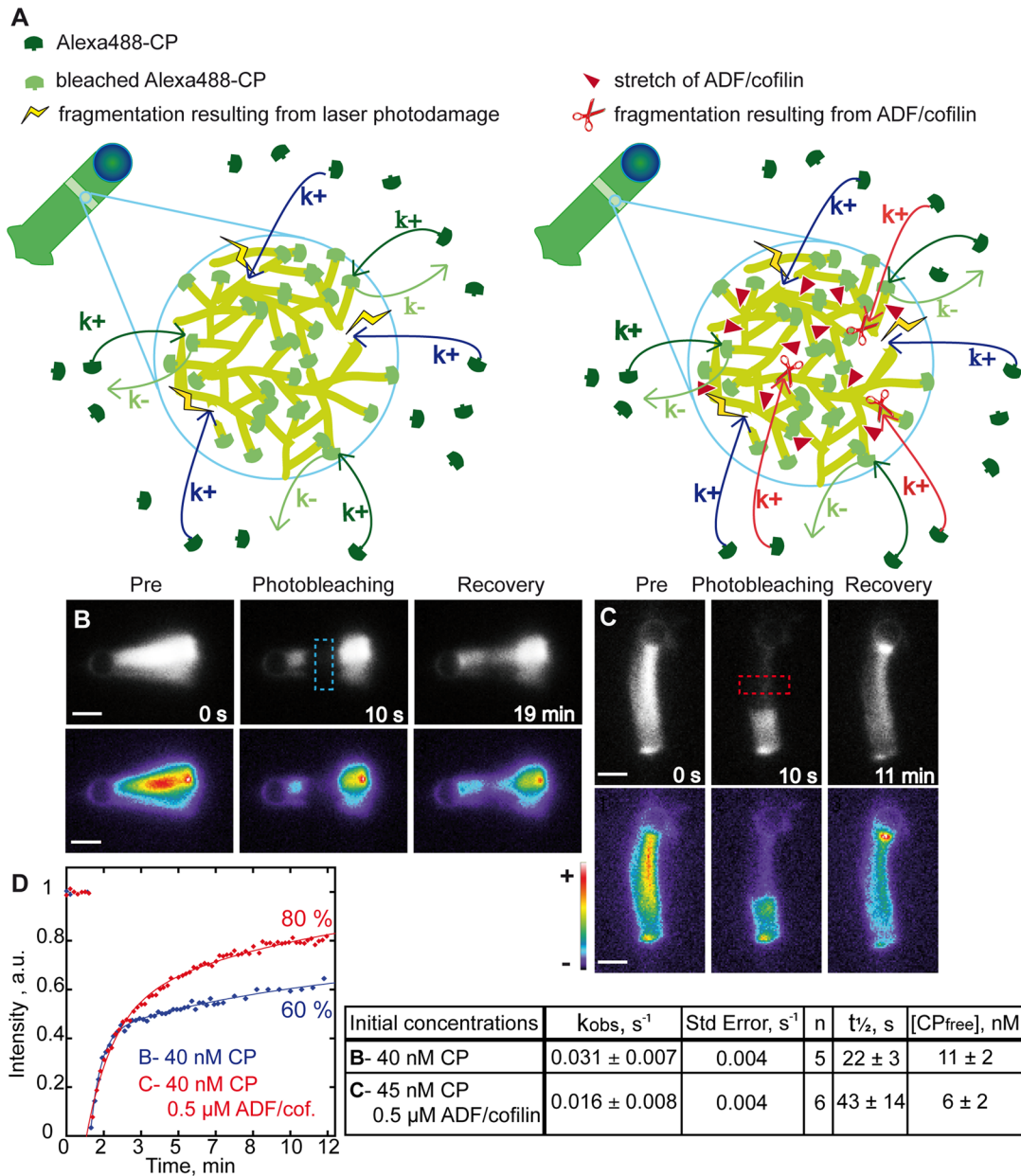


FIGURE 4: ADF/cofilin severs short actin filaments and creates new filament barbed ends during reconstituted bead motility. (A) Schematic representation of the photobleaching experiments of Alexa Fluor 488-labeled CP in a dense actin network nucleated from the pWA-coated beads in the absence of ADF/cofilin (left) and in the presence of ADF/cofilin (right). Once dissociated from the end of filaments according to its kinetic dissociation constant k_- (limiting step), bleached CP is rapidly replaced by unbleached Alexa Fluor 488-CP diffusing from the surrounding medium (following a kinetic constant equal to its association constant rate k_+ multiplied by the protein concentration in the medium). Filaments are also damaged and fragmented by the laser light during the photobleaching process. These new artificial barbed ends are rapidly capped. In the presence of ADF/cofilin, filaments are further fragmented, leading to the rapid recruitment of CP. (B and C) Time-lapse images of FRAP experiments of Alexa Fluor 488-CP on the propulsive actin network nucleated from GST-pWA-coated beads in the absence (A) or presence (B) of 0.3 μ M Alexa Fluor 568-ADF/cofilin under conditions similar to Figure 2A. Images were taken at the indicated times during polymerization. Time-lapse images were acquired by fluorescence microscopy. The photobleached zones, indicated by a dashed rectangle on the images, were obtained by a local intense laser illumination. For a better visualization of CP fluorescence intensity, images are also shown in pseudocolor. Scale bar: 5 μ m. (D) Graph representing the time course of fluorescence intensity changes for Alexa Fluor 488-labeled CP within the bleached zones. For an easier comparison, data were normalized by fluorescence intensity prior to bleaching. Blue, data corresponding to the experiment shown in (B) in the absence of ADF/cofilin; red, those corresponding to experiment (C) in the presence of ADF/cofilin. Means and statistics obtained for the kinetics of the fluorescence recovery after photobleaching of Alexa Fluor 488-CP in different experiments are presented. Curve fits were obtained using a double exponential function in KaleidaGraph. The dissociation constant was fixed to the mean experimental value found ($k_- = 0.00155 s^{-1}$) in order to solve the other kinetic constant k_{obs} , therefore permitting the calculation of the half-time $t_{1/2}$ and the free concentration of CP in the medium (using $k_{+th} = 3 \mu M^{-1} \cdot s^{-1}$). Data are represented as mean \pm SE. (See also Movie S5.)

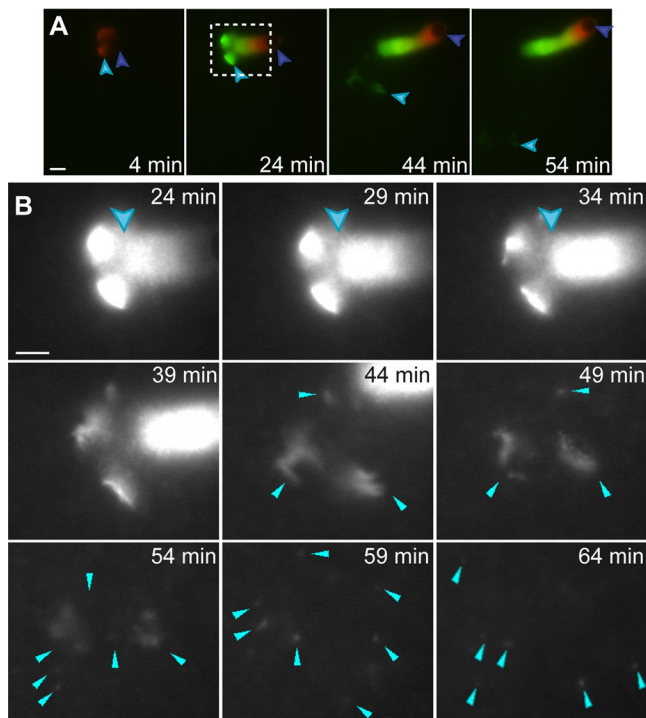


FIGURE 5: Evidence for the macroscopic stochastic dynamics of ADF/cofilin severing activity. (A) GST-pWA-coated beads were added to a motility medium containing 4 μM Alexa Fluor 568-actin monomers, 150 nM Arp2/3 complex, 25 nM CP, and 0.6 μM Alexa Fluor 488-ADF/cofilin under the same conditions as in Figure 2A. The dark blue arrowhead points to the motile bead and the light blue arrowhead follows the thick actin shell assembled prior to symmetry breaking and its fragmentation into small meshwork pieces. Alexa Fluor 568-actin is colored in red, and Alexa Fluor 488-ADF/cofilin in green. (B) is a magnification of the area outlined by a dashed box in (A). The signal in (B) corresponds to fluorescence of Alexa Fluor 568-actin only. Scale bar: 5 μm . (See also Movie S6.)

(Schafer *et al.*, 1996), the double exponential fits of the fluorescence recovery curves revealed 29 nM of CP was bound to actin comet tail in the absence of ADF/cofilin, corresponding to 73% of the initial concentration of CP, whereas 39 nM CP was bound in the presence of ADF/cofilin, corresponding to 87% of the initial concentration of CP (Figure 4). This difference of 10 nM CP_{bound} represents the concentration of free barbed ends created by ADF/cofilin-severing activity within the actin network.

Since we knew the concentration of ADF/cofilin present in the medium and the increased number of barbed ends resulting from fragmentation by ADF/cofilin, we estimated the efficiency of severing by ADF/cofilin as at least one severing event per 100 molecules of ADF/cofilin present.

ADF/cofilin is required for the macroscopic release of the aged end of the comet tail

To investigate whether severing of individual actin filaments by ADF/cofilin leads to a macroscopic dissociation and disassembly of the Arp2/3 complex-mediated network, we reconstituted motility of functionalized beads with a high concentration of ADF/cofilin (0.6 μM), and tracked the distribution of fluorescently labeled actin and ADF/cofilin (Figure 5A and Movie S6). The spatial and temporal incorporation of both proteins was in agreement with those presented in Figure 2. Remarkably, under these experimental conditions, we observed that the oldest actin region, which consists of the

dense actin shell assembled prior to symmetry breaking, broke into small pieces of meshwork that drifted away and disappeared in the medium (Figure 5B). Paradoxically, in the absence of ADF/cofilin in the motility medium, the oldest actin region remained intact throughout the duration of the experiments (Figure 1). Given both the microscopic severing activity of ADF/cofilin highlighted by the FRAP experiments (Figure 4) and its spatiotemporal localization, we propose, in the minimal experimental context of our study involving Arp2/3 complex, CP, and ADF/cofilin, that the release of portions of the actin-branched network is due to a macroscopic destabilization modulated by actin filament severing by ADF/cofilin. Consequently, the disassembly of the actin comet tails appears inconsistent with a treadmilling mechanism wherein the actin network turnover results only from the depolymerization of actin filaments from their pointed ends. Instead, the rapid and macroscopic release of the aged actin network seems likely related to the process of stochastic fragmentation mediated by ADF/cofilin recently described at the single-filament level (Michelot *et al.*, 2007; Roland *et al.*, 2008; Staiger *et al.*, 2009).

DISCUSSION

The actin cytoskeleton is a highly dynamic array and its mechanical properties are involved in many essential cellular functions like cell division, polarity, morphogenesis, and motility (Pollard and Cooper, 2009). To engage in such complex behaviors, cells maintain precise control over the spatial and temporal localization of actin polymerization (Rohatgi *et al.*, 1999), and finely modulate the actin filament networks' mechanical properties in response to extracellular stimuli. In this study, we used a reconstituted motility system and followed in space and time the incorporation of three key actin-binding proteins (Arp2/3 complex, CP, and ADF/cofilin) within a dynamic actin network to provide insights into the establishment of a mechanochemical gradient along this actin network during particle propulsion. Our findings reveal that ADF/cofilin orchestrates the mechanical destabilization of actin networks during motility, leading to the macroscopic loss of portions of the network to the medium, whereas CP coordinates the spatiotemporal localization of ADF/cofilin. Thus these two proteins act in concert to modulate the biomechanical properties and the turnover of actin filament arrays during actin-based motility by branched networks.

CP orchestrates the spatiotemporal localization of ADF/cofilin within propulsive networks

Heterodimeric capping protein has a high association rate constant and can rapidly block the fast-growing barbed ends of actin filaments (Schafer *et al.*, 1996). Thus CP efficiently prevents filament elongation at locations distal to nucleation sites, which are thought to exist near propulsion sites (Rohatgi *et al.*, 1999; Pantaloni *et al.*, 2000; Iwasa and Mullins, 2007). Accordingly, our results revealed that the spatiotemporal incorporation of CP was superimposed on that of actin. This suggests that actin filament branches initiated by the Arp2/3 complex at the nucleation sites (i.e., the bead surface) elongate soon after nucleation for a only brief period before being capped (Figures 1 and 4; Achard *et al.*, 2010). Therefore CP restricts the "active" zone (where new actin monomers are inserted; Akin and Mullins, 2008; Achard *et al.*, 2010; Reymann *et al.*, 2010) to the vicinity of nucleation sites and controls the chronological and spatial progression of the "dead" zone (where actin filament elongation has ceased) along the propulsive actin meshwork. This mechanism yields a macroscopic gradient of nucleotide-loaded states along the actin filament network. Indeed, since actin monomers are added only near the

bead surface, ATP-loaded subunits are temporarily constrained to this region of the comet tail before ATP hydrolysis and phosphate dissociation occur in the whole network. Because ADF/cofilin has a marked preference for ADP-loaded actin (Blanchoin and Pollard, 1999), the establishment of this gradient controls the gradual incorporation of ADF/cofilin along the actin network (Figures 2A and 3). In addition, by increasing the rate of phosphate release, ADF/cofilin limits the size of the actin filament network resistant to its interaction (Blanchoin and Pollard, 1999; Suarez *et al.*, 2011). Consistent with this scheme, as soon as bead motility stops (Figure 2B), due to a lack of actin monomers in solution, the size of the ADF/cofilin exclusion zone around the bead rapidly decreases, and ultimately disappears after 1 h. The spatiotemporal localization of CP and ADF/cofilin described here is fully consistent with their mutual distribution in vivo (Svitkina and Borisy, 1999; Okreglak and Drubin, 2007). Indeed, CP localizes to the lamellipodium in the 1 μm immediately adjacent to the plasma membrane (Iwasa and Mullins, 2007), whereas ADF/cofilin is excluded from 0.2–0.7 μm of the lamellipodial network (Svitkina and Borisy, 1999). Our present results demonstrate that the gradient of ADF/cofilin along the actin network is controlled by kinetics, that is, by its higher affinity for ADP-loaded subunits and its ability to accelerate P_i release (Figures 2 and 3).

ADF/cofilin catalyzes the microscopic severing and macroscopic destabilization of dense and rigid actin networks

In terms of its mechanical properties, the propulsive actin filament network is made of a dense and rigid actin filament array with an elongation zone restricted spatially and temporally to the vicinity of the nucleation particle. The FRAP experiments provide evidence that ADF/cofilin was able to sever actin filaments within this stiff and highly cross-linked actin network, as the actin-based propulsion of particles was achieved in the presence of a critical amount of CP. This also emphasized that actin filament severing by ADF/cofilin, followed by the rapid recruitment of CP to newly created barbed ends, introduces a mechanical heterogeneity throughout branched networks. The microscopic fragmentation of actin filaments by ADF/cofilin within the comet tail is consistent with the fact that its spatial and temporal incorporation correlated with the decrease of actin filament density along the aging regions of the tail (Figure 2, A and D, line scans). In addition, studies have established that ADF/cofilin also dissociates Arp2/3-generated actin filament branches (Blanchoin *et al.*, 2000a; Chan *et al.*, 2009) and only slightly affects the rate of depolymerization of actin filaments (Andrianantoandro and Pollard, 2006; Suarez *et al.*, 2011). Thus a global process that relies on filament debranching and severing by ADF/cofilin, rather than enhanced pointed-end depolymerization, is an attractive explanation for the loss of actin mass from older regions of an actin array that is dense and rigid (Figures 2A, line scans, and 3C). We propose that loss of actin filaments in the comet tail due to fragmentation by ADF/cofilin occurs in two steps: 1) it happens microscopically at the single actin filament level, and 2) it propagates macroscopically to release stochastically not single filaments but large portions of the aged actin network. This model is in agreement with the fast disassembly of actin filaments within dense branched networks in endocytic patches (Berro *et al.*, 2010). Furthermore, it reconciles the paradox for the apparent dissociation rate of CP being three orders of magnitude faster in vivo compared with in vitro in the absence of any severing protein (Miyoshi *et al.*, 2006).

Concluding remarks

The rapid and continuous recruitment of CP throughout the Arp2/3-mediated actin assembly imposes mechanical properties on the actin network conformation, which is a rigid array necessary for the production of protrusive force. CP also directly controls the spatiotemporal recruitment of ADF/cofilin, which in turn affects the actin network mechanics and CP turnover. Consequently, we propose that the synergy between CP and ADF/cofilin leads to a tight coupling between both the biochemical and mechanical properties of the actin networks, which explains the turnover of actin filaments at the leading edge of motile cells (Svitkina and Borisy, 1999).

It must be kept in mind that cells display an infinite complexity and the spatiotemporal distribution of actin networks' aging zones imposed by CP, together with the subsequent actin monomer recycling by ADF/cofilin severing activity, are modulated by a diverse battery of regulating proteins, including Aip1 (Kueh *et al.*, 2008; Okreglak and Drubin, 2010), coronin (Gandhi *et al.*, 2009), tropomyosin (Blanchoin *et al.*, 2001; Bugyi *et al.*, 2010), and myosin II (Hotulainen and Lappalainen, 2006). In addition, processive actin polymerases such as formin (Hotulainen and Lappalainen, 2006; Lee *et al.*, 2010) or Enabled/vasodilator-stimulated phosphoprotein (Ena/VASP) family of proteins (Bear, 2002; Trichet *et al.*, 2007; Hansen and Mullins, 2010) protect actin filament barbed ends against CP and generate parallel actin networks with specific mechanical properties. Further understanding of the interplay between the control of actin dynamics and the actin network's mechanical properties should come from studies where the minimal reconstituted motility system is expanded to include the presence of additional actin-regulating factors.

MATERIALS AND METHODS

Protein production and labeling

Actin was purified from rabbit skeletal muscle acetone powder (Spudich and Watt, 1971). Monomeric Ca-ATP-actin was purified by gel-filtration chromatography on Sephacryl S-300 (McLean-Fletcher and Pollard, 1980) at 4°C in G buffer (5 mM Tris-HCl, pH 8.0, 0.2 mM ATP, 0.1 mM CaCl_2 , and 0.5 mM dithiothreitol [DTT]). Actin was labeled on lysines with Alexa Fluor 568 or Alexa Fluor 488 as described previously (Isambert *et al.*, 1995; Egile *et al.*, 1999). The Arp2/3 complex was purified from bovine brain extracts according to Egile *et al.* (1999). GST-WA, GST-pWA, human profilin, mouse CP, and ADF/cofilin were expressed and purified as described previously (Almo *et al.*, 1994; Machesky *et al.*, 1999; Blanchoin *et al.*, 2000b; Falck *et al.*, 2004). The Arp2/3 complex, CP, and ADF/cofilin were labeled on cysteines with Alexa Fluor 568 or Alexa Fluor 488. D34C, C62A mutations were introduced on *COF1 Saccharomyces cerevisiae* cofilin gene, as previously described (Lappalainen *et al.*, 1997). We referred to this double mutant protein as "D34C-ADF/cofilin" and labeled it on C34 (Suarez *et al.*, 2011). The purified protein solution was dialyzed overnight against two changes of dialysis buffer (10 mM Tris-HCl, pH 7.5, 150 mM NaCl, 2 mM EDTA, 2 mM Tris(2-carboxyethyl)phosphine hydrochloride [TCEP]). The protein concentration was then adjusted to 100 μM for a total volume of 1 ml and labeled overnight with sixfold excess of Alexa 488 or Alexa 568 C5-maleimide (Invitrogen, Carlsbad, CA). Alexa Fluor 488- or Alexa Fluor 568-protein was purified by gel-filtration chromatography on G25 (Sigma-Aldrich, St. Louis, MO) in elution buffer (10 mM Tris-HCl, pH 7.5, 150 mM NaCl, 2 mM EDTA, 2 mM DTT) and stored at -80°C .

Coating of beads

Carboxylate polystyrene microspheres (4.5 μm diameter, 2.6% solids-latex suspension; Polysciences, Eppelheim, Germany) were

mixed with 2 μM GST-pWA in X buffer (10 mM HEPES, pH 7.5, 0.1 M KCl, 1 mM MgCl_2 , 1 mM ATP, and 0.1 mM CaCl_2) for 15 min at 20°C on a thermoshaker. The beads coated with pWA were then washed in X buffer containing 1% bovine serum albumin (BSA) and stored on ice for 48 h in X buffer-0.1% BSA. GST-pWA surface density on the beads was quantified on SDS-PAGE gel: 2.4×10^4 pWA/ μm^2 .

Motility assay

GST-pWA-coated beads were mixed with a motility medium containing 4 μM actin monomers, 12 μM profilin, and the indicated concentration of Arp2/3, CP, and ADF/cofilin, labeled or not, in X buffer (10 mM HEPES, pH 7.0, 0.1 M KCl, 1 mM MgCl_2 , 1 mM ATP, and 0.1 mM CaCl_2) supplemented with 1% BSA, 0.2% methylcellulose, 3 mM DTT, 0.13 mM DABCO, 1.8 mM ATP. Image acquisition was performed on a Zeiss axioplan microscope (Jena, Germany) equipped with a 63 \times , 1.5 numerical aperture Plan-APOCHROMAT objective lens, and images were collected with a Hamamatsu ORCA CCD camera (Hamamatsu, Herrsching am Ammersee, Germany) with Metavue version 6.2r6 (Universal Imaging, Media, PA). Two sets of filters were used: FITC filter (BP 450–490, FT 510, BP 515–568, Zeiss) adapted to the Alexa Fluor 488 and rhodamine filter (BP 546/12, FT580, LP 590, Zeiss) adapted to the Alexa Fluor 568. A journal was created in Metavue in order to acquire three images quasi-simultaneously (phase contrast, Alexa Fluor 568 acquisition, Alexa Fluor 488 acquisition).

For bead motility, time-lapse images of motile beads were acquired quasi-simultaneously by fluorescence microscopy with two sets of filters adapted to Alexa Fluor 488 and Alexa Fluor 568, permitting the tracking of two proteins.

Data analysis of FRAP experiments

Images were then combined using Metamorph (Molecular Devices, Sunnyvale, CA). Images corresponding to the different fluorophores were color combined and analyzed (line scan, threshold area) using Metamorph version 7.5. Data were then analyzed (normalization, curve fits) and plotted with KaleidaGraph version 4.01 (Synergy Software, Reading, PA). For the fluorescence recoveries after bleaching, double exponential curve fits were first achieved on experiments in the absence of ADF/cofilin in order to obtain a mean value of the k_- ($0.00155 \text{ s}^{-1} \pm 0.00016$; $n = 5$). This value was then fixed in all double exponential fits possible to obtain the other kinetic constant ($k_{\text{obs}} = k_+ * [\text{CP}_{\text{free}}]$). Using the theoretical k_+ ($3 \mu\text{M}^{-1} \text{ s}^{-1}$) published by Schafer *et al.* (1996), we obtained an estimation of the concentration of free CP in the medium.

ACKNOWLEDGMENTS

This work was supported by grants to L.B. from Agence Nationale de la Recherche (ANR-08-BLAN-0012 and ANR-08-SYSC-013) and a fellowship to A.C.R. from CEA. C.J.S. was supported by the Physical Biosciences Program of the Office of Basic Energy Sciences, U. S. Department of Energy, under contract number DE-FG02-04ER15526.

REFERENCES

- Achard V, Martiel JL, Michelot A, Guerin C, Reymann AC, Blanchoin L, Boujemaa-Paterski R (2010). A "primer"-based mechanism underlies branched actin filament network formation and motility. *Curr Biol* 20, 423–428.
- Akin O, Mullins RD (2008). Capping protein increases the rate of actin-based motility by promoting filament nucleation by the Arp2/3 complex. *Cell* 133, 841–851.
- Almo SC, Pollard TD, Way M, Lattman EE (1994). Purification, characterization and crystallization of *Acanthamoeba* profilin expressed in *Escherichia coli*. *J Mol Biol* 236, 950–952.
- Andrianantoandro E, Pollard TD (2006). Mechanism of actin filament turnover by severing and nucleation at different concentrations of ADF/cofilin. *Mol Cell* 24, 13–23.
- Bear JE (2002). Formins: taking a ride on the barbed end. *Dev Cell* 3, 149–150.
- Bernstein BW, Bamburg JR (2010). ADF/cofilin: a functional node in cell biology. *Trends Cell Biol* 20, 187–195.
- Berro J, Sirotkin V, Pollard TD (2010). Mathematical modeling of endocytic actin patch kinetics in fission yeast: disassembly requires release of actin filament fragments. *Mol Biol Cell* 21, 2905–2915.
- Blanchoin L, Pollard TD (1999). Mechanism of interaction of *Acanthamoeba* actophorin (ADF/cofilin) with actin filaments. *J Biol Chem* 274, 15538–15546.
- Blanchoin L, Pollard TD, Hitchcock-DeGregori SE (2001). Inhibition of the Arp2/3 complex-nucleated actin polymerization and branch formation by tropomyosin. *Curr Biol* 11, 1300–1304.
- Blanchoin L, Pollard TD, Mullins RD (2000a). Interaction of ADF/cofilin, Arp2/3 complex, capping protein and profilin in remodeling of branched actin filament networks. *Curr Biol* 10, 1273–1282.
- Blanchoin L, Robinson RC, Choe S, Pollard TD (2000b). Phosphorylation of *Acanthamoeba* actophorin (ADF/cofilin) blocks interaction with actin without a change in atomic structure. *J Mol Biol* 295, 203–211.
- Brieher WM, Kueh HY, Ballif BA, Mitchison TJ (2006). Rapid actin monomer-insensitive depolymerization of *Listeria* actin comet tails by cofilin, coronin, and Aip1. *J Cell Biol* 175, 315–324.
- Bugyi B, Didry D, Carlier MF (2010). How tropomyosin regulates lamellipodial actin-based motility: a combined biochemical and reconstituted motility approach. *EMBO J* 29, 14–26.
- Carlier MF, Laurent V, Santolini J, Melki R, Didry D, Xia GX, Hong Y, Chua NH, Pantaloni D (1997). Actin depolymerizing factor (ADF/cofilin) enhances the rate of filament turnover: implication in actin-based motility. *J Cell Biol* 136, 1307–1322.
- Chan C, Beltzner CC, Pollard TD (2009). Cofilin dissociates Arp2/3 complex and branches from actin filaments. *Curr Biol* 19, 537–545.
- Chhabra ES, Higgs HN (2007). The many faces of actin: matching assembly factors with cellular structures. *Nat Cell Biol* 9, 1110–1121.
- Cooper JA, Schafer DA (2000). Control of actin assembly and disassembly at filament ends. *Curr Opin Cell Biol* 12, 97–103.
- De La Cruz EM (2005). Cofilin binding to muscle and non-muscle actin filaments: isoform-dependent cooperative interactions. *J Mol Biol* 346, 557–564.
- De La Cruz EM (2009). How cofilin severs an actin filament. *Biophys Rev* 1, 51–59.
- Egile C, Loisel TP, Laurent V, Li R, Pantaloni D, Sansonetti PJ, Carlier MF (1999). Activation of the CDC42 effector N-WASP by the *Shigella flexneri* IcsA protein promotes actin nucleation by Arp2/3 complex and bacterial actin-based motility. *J Cell Biol* 146, 1319–1332.
- Falck S, Paavilainen VO, Wear MA, Grossmann JG, Cooper JA, Lappalainen P (2004). Biological role and structural mechanism of twinfilin-capping protein interaction. *EMBO J* 23, 3010–3019.
- Gandhi M, Achard V, Blanchoin L, Goode BL (2009). Coronin switches roles in actin disassembly depending on the nucleotide state of actin. *Mol Cell* 34, 364–374.
- Goley ED, Welch MD (2006). The ARP2/3 complex: an actin nucleator comes of age. *Nat Rev Mol Cell Biol* 7, 713–726.
- Hansen SD, Mullins RD (2010). VASP is a processive actin polymerase that requires monomeric actin for barbed end association. *J Cell Biol* 191, 571–584.
- Hotulainen P, Lappalainen P (2006). Stress fibers are generated by two distinct actin assembly mechanisms in motile cells. *J Cell Biol* 173, 383–394.
- Isambert H, Venier P, Maggs AC, Fattoum A, Kassab R, Pantaloni D, Carlier MF (1995). Flexibility of actin filaments derived from thermal fluctuations. Effect of bound nucleotide, phalloidin, and muscle regulatory proteins. *J Biol Chem* 270, 11437–11444.
- Iwasa JH, Mullins RD (2007). Spatial and temporal relationships between actin-filament nucleation, capping, and disassembly. *Curr Biol* 17, 395–406.
- Kim K, Yamashita A, Wear MA, Maeda Y, Cooper JA (2004). Capping protein binding to actin in yeast: biochemical mechanism and physiological relevance. *J Cell Biol* 164, 567–580.
- Kueh HY, Charras GT, Mitchison TJ, Brieher WM (2008). Actin disassembly by cofilin, coronin, and Aip1 occurs in bursts and is inhibited by barbed-end cappers. *J Cell Biol* 182, 341–353.
- Kuhn JR, Pollard TD (2007). Single molecule kinetic analysis of actin filament capping. Polyphosphoinositides do not dissociate capping proteins. *J Biol Chem* 282, 28014–28024.

- Lappalainen P, Fedorov EV, Fedorov AA, Almo SC, Drubin DG (1997). Essential functions and actin-binding surfaces of yeast cofilin revealed by systematic mutagenesis. *EMBO J* 16, 5520–5530.
- Lee K, Gallop JL, Rambani K, Kirschner MW (2010). Self-assembly of filopodia-like structures on supported lipid bilayers. *Science* 329, 1341–1345.
- Loisel TP, Boujemaa R, Pantaloni D, Carlier MF (1999). Reconstitution of actin-based motility of *Listeria* and *Shigella* using pure proteins. *Nature* 401, 613–616.
- Machesky LM, Mullins DM, Higgs HN, Kaiser DA, Blanchoin L, May RC, Hall ME, Pollard TD (1999). Scar, a WASP-related protein, activates nucleation of actin filaments by the Arp2/3 complex. *Proc Natl Acad Sci USA* 96, 3739–3744.
- Maciver SK, Zot HG, Pollard TD (1991). Characterization of actin filament severing by actophorin from *Acanthamoeba castellanii*. *J Cell Biol* 115, 1611–1620.
- Martin AC, Welch MD, Drubin DG (2006). Arp2/3 ATP hydrolysis-catalysed branch dissociation is critical for endocytic force generation. *Nat Cell Biol* 8, 826–833.
- McCullough BR, Blanchoin L, Martiel JL, De la Cruz EM (2008). Cofilin increases the bending flexibility of actin filaments: implications for severing and cell mechanics. *J Mol Biol* 381, 550–558.
- McGough A, Pope B, Chiu W, Weeds A (1997). Cofilin changes the twist of F-actin: implications for actin filament dynamics and cellular function. *J Cell Biol* 138, 771–781.
- McLean-Fletcher S, Pollard TD (1980). Identification of a factor in conventional muscle actin preparations which inhibits actin filament self-association. *Biochem Biophys Res Commun* 96, 18–27.
- Michelot A, Berro J, Guerin C, Boujemaa-Paterski R, Staiger CJ, Martiel JL, Blanchoin L (2007). Actin-filament stochastic dynamics mediated by ADF/cofilin. *Curr Biol* 17, 825–833.
- Miyoshi T, Tsuji T, Higashida C, Hertzog M, Fujita A, Narumiya S, Scita G, Watanabe N (2006). Actin turnover-dependent fast dissociation of capping protein in the dendritic nucleation actin network: evidence of frequent filament severing. *J Cell Biol* 175, 947–955.
- Mullins RD, Heuser JA, Pollard TD (1998). The interaction of Arp2/3 complex with actin: nucleation, high-affinity pointed end capping, and formation of branching networks of filaments. *Proc Natl Acad Sci USA* 95, 6181–6186.
- Okada K, Ravi H, Smith EM, Goode BL (2006). Aip1 and cofilin promote rapid turnover of yeast actin patches and cables: a coordinated mechanism for severing and capping filaments. *Mol Biol Cell* 17, 2855–2868.
- Okreglak V, Drubin DG (2007). Cofilin recruitment and function during actin-mediated endocytosis dictated by actin nucleotide state. *J Cell Biol* 178, 1251–1264.
- Okreglak V, Drubin DG (2010). Loss of Aip1 reveals a role in maintaining the actin monomer pool and an in vivo oligomer assembly pathway. *J Cell Biol* 188, 769–777.
- Pantaloni D, Boujemaa R, Didry D, Gounon P, Carlier M-F (2000). The Arp2/3 complex branches filament barbed ends: functional antagonism with capping proteins. *Nat Cell Biol* 2, 385–391.
- Pollard TD, Blanchoin L, Mullins RD (2000). Molecular mechanisms controlling actin filament dynamics in nonmuscle cells. *Annu Rev Biophys* 29, 545–576.
- Pollard TD, Borisy GG (2003). Cellular motility driven by assembly and disassembly of actin filaments. *Cell* 112, 453–465.
- Pollard TD, Cooper JA (2009). Actin, a central player in cell shape and movement. *Science* 326, 1208–1212.
- Reymann A-C, Martiel J-L, Cambier T, Blanchoin L, Boujemaa-Paterski R, Théry M (2010). Nucleation geometry governs ordered actin networks structures. *Nat Mat* 9, 827–832.
- Rohatgi R, Ma L, Miki H, Lopez M, Kirchhausen T, Takenawa T, Kirschner MW (1999). The interaction between N-WASP and the Arp2/3 complex links Cdc42-dependent signals to actin assembly. *Cell* 97, 221–231.
- Roland J, Berro J, Michelot A, Blanchoin L, Martiel JL (2008). Stochastic severing of actin filaments by actin depolymerizing factor/cofilin controls the emergence of a steady dynamical regime. *Biophys J* 94, 2082–2094.
- Rouiller I, Xu XP, Amann KJ, Egile C, Nickell S, Nicastro D, Li R, Pollard TD, Volkman N, Hanein D (2008). The structural basis of actin filament branching by the Arp2/3 complex. *J Cell Biol* 180, 887–895.
- Schafer DA, Jennings PB, Cooper JA (1996). Dynamics of capping protein and actin assembly in vitro: uncapping barbed ends by polyphosphoinositides. *J Cell Biol* 135, 169–179.
- Spudich JA, Watt S (1971). The regulation of rabbit skeletal muscle contraction. I. Biochemical studies of the interaction of the tropomyosin-troponin complex with actin and the proteolytic fragments of myosin. *J Biol Chem* 246, 4866–4871.
- Staiger CJ, Sheahan MB, Khurana P, Wang X, McCurdy DW, Blanchoin L (2009). Actin filament dynamics are dominated by rapid growth and severing activity in the *Arabidopsis* cortical array. *J Cell Biol* 184, 269–280.
- Suarez C, Roland J, Boujemaa-Paterski R, Kang H, McCullough BR, Reymann AC, Guérin C, Martiel JL, De La Cruz E, Blanchoin L (2011). Cofilin tunes the nucleotide state of actin filaments and severs at bare and decorated segment boundaries. *Curr Biol* 21, 862–868.
- Svitkina TM, Borisy GG (1999). Arp2/3 complex and actin depolymerizing factor/cofilin in dendritic organization and treadmilling of actin filament array in lamellipodia. *J Cell Biol* 145, 1009–1026.
- Trichet L, Campas O, Sykes C, Plastino J (2007). VASP governs actin dynamics by modulating filament anchoring. *Biophys J* 92, 1081–1089.
- van der Gucht J, Paluch E, Plastino J, Sykes C (2005). Stress release drives symmetry breaking for actin-based movement. *Proc Natl Acad Sci USA* 102, 7847–7852.
- Welch MD, Rosenblatt J, Skoble J, Portnoy DA, Mitchison TJ (1998). Interaction of human Arp2/3 complex and the *Listeria monocytogenes* ActA protein in actin filament nucleation. *Science* 281, 105–108.
- Yamashita A, Maeda K, Maeda Y (2003). Crystal structure of CapZ: structural basis for actin filament barbed end capping. *EMBO J* 22, 1529–1538.